Reconstruction of the Very Early Thalamo-Cortical Network with Combined EEG and MEG on Realistic Head Modeling

Konstantinos Politof, Marios Antonakakis, *Member, IEEE*, Andreas Wollbrink, Carsten H. Wolters, Michalis Zervakis, *Member, IEEE*

***Abstract*—The early primary somatosensory network remains a rarely investigated brain area due to the fast transitions among the involved cortical and subcortical regions. In this regard, a non-invasive and subject-specific method that quantifies the very early temporal interdependences in the thalamo-cortical/cortico-cortical pathway of the primary somatosensory network would be of particular significance. Combined electro- (EEG) and magneto- (MEG) encephalography (EMEG) source analysis has been shown to exploit the complementary content of the single modalities EEG and MEG based on subject-specific and realistic head modeling. The current study aims to investigate the connectivity of the very early primary somatosensory network using EMEG source analysis with functionally-based decomposition and time-variant effective connectivity. Three-time temporally determined components are chosen based on the combined somatosensory evoked responses to highlight the thalamo-cortical and cortico-cortical interactions. The results confirm that electrophysiological activity flows from the thalamic regions of the brain to the first tangentially oriented neurological somatosensory brain region (Broadman area 3b, thalamo-cortical connection) and then to the radially-oriented brain region (Broadman area 3a, cortico-cortical connection). We also present that the flows between the investigated components that do not fit to the flow of the neurological activity from the wrist to the somatosensory network, when increasing the confidence interval (CI). Overall, EMEG source analysis with realistic head modeling and a functionally-based connectivity estimator is able to capture very fast transitions on the early-involved somatosensory network.**

I. Introduction

EEG and MEG are two measurement modalities that offer high temporal resolution ((sub)millisecond range) and thus offer a non-invasive way to study fast temporal connectivity networks in the human brain. The early primary somatosensory network (including thalamic structures and the primary somatosensory cortex (SI)) is a challenging network, with a small number of studies having investigate it [1, 2, 3, 4]. The modeling of such a network can interpret better the use of SI network that offers high Signal-to-Noise Ratio (SNR) somatosensory evoked potentials (SEP) in EEG or fields (SEF) in MEG [1]. This network is able to serve as entry point for developing complex pipelines [5, 6] or sensitivity studies [7, 8]. In this study, we focus on the estimation of the very early primary somatosensory network including (1) the thalamic component (P14), and (2) the first and second transient components P20/N20 and P25/N25, respectively.

Recently, the combination of EEG and MEG in source analysis has enabled precise event localization, for example in epilepsy [9, 10] or in somatosensory research [7, 11] due to the complementary content that EMEG preserves from both EEG and MEG [12, 13]. This combination exploits the insensitivity of MEG to inter-individual skull conductivity variations while preserving the accurate EEG indication of orientation [7]. However, due to the large inter-subject variability of skull conductivity, EEG is far more sensitive to skull conductivity variations, so that the estimation of individual skull conductivity becomes a crucial factor [6, 14]. In this work, we overcome this limitation by using a calibration procedure, where individual skull conductivity is estimated based on a two-level calibration procedure including an individual model for white matter conductivity anisotropy using diffusion tensor Magnetic Resonance Imaging (DTI) data [6]. Therefore, we utilize the complementary characteristics of EEG and MEG within a individually calibrated head model for accurately investigating the time-variant alterations in the primary somatosensory network.

Over the last decades, it has been shown that the early SEP/SEF responses are temporally very close to each other [1, 2, 3], making the use of a decomposition method quite important before any attempt to reconstruct the time-variant content of the early primary somatosensory network. In this regard, functional source separation (FSS) is a decomposition technique that belongs to the family of blind source separation approaches and has been applied in SEP/SEF [15, 16] and recently in combined SEP/SEF [17]. In this study, we make use of the FSS algorithm for the decomposition of the SEP/SEF responses into the components of interest, i.e., P14, P20/N20 and P25/N25.

Since our attempt focuses on the investigation of early stage interactions among the thalamo-cortical and cortico-cortical pathways, we employ the Generalized Orthogonalized Partial Directed Coherence – GOPDC as connectivity estimator. GOPDC diminishes the co-variability due to spatial smearing [18]. A statistical filtering of the estimated flows is also performed based on surrogate analysis, investigating the influence of confidence interval on the estimation of the network by the use of two different CI, i.e., 90 % and 95 %.

The description of data and methodological approaches is illustrated in Section II. The results of the study are presented in Section III, followed by a discussion and the outlook in Section IV.

K. P. (corresponding author, email:kpolitof@isc.tuc.gr) and M. Z. are with the School of Electrical and Computer Engineering, Technical University of Crete, Chania, Greece. M. A. (equally contributed), A. W. and C. H. W. are with the Institute for Biomagnetism and Biosignalanalysis, University of Münster, Münster, Germany.

II. Participant and Methods

A. Experiment setup and Measurement Preprocessing

A healthy volunteer (32 years old) participated in somatosensory experiment, undergoing median nerve stimulation at the right wrist. The stimulus strength was adjusted until a clear movement of the thumb was observed. The inter-stimulus interval (ISI) was 400 ms with a random deviation of 50 ms to avoid habituation. We used a pulse duration of 0.5 ms. The entire measurement session was ten minutes long. Simultaneous EEG/MEG measurements were acquired with a sampling frequency of 1200 Hz. The EEG system consisted of 80 electrodes, and the MEG system (VMS MedTech Ltd) was comprised of 275 first order axial gradiometers. The volunteer also underwent a 3T MAGNETOM MRI (Siemens Medical Solutions) to measure its T1, T2 and diffusion-weighted MR (dMRI) images of 1 mm and 1.9 mm resolution, respectively.

The first step of analysis was the preprocessing of the raw EEG/MEG recordings using the MATLAB toolbox FieldTrip [19]. A band-pass filter of 20-250 Hz and a Notch filter suppressing the power line noise of 50 Hz (and its harmonics) were applied. The defined window of each trial was from -100 to 200 ms.

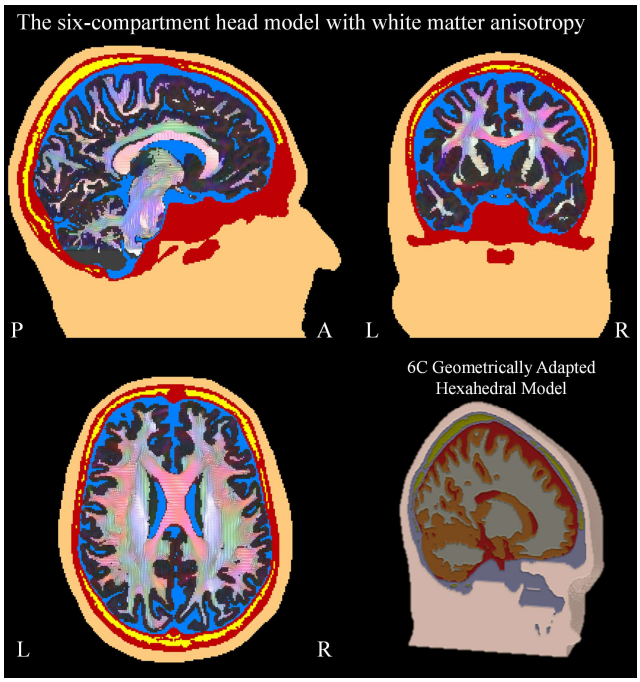

Fig. 1. Segmented 6C model (upper row: midsagittal and midcoronal view, left lower column; midaxial view). The compartments are colored as follows: scalp in light leather color, skull compacta in dark red, skull spongiosa in yellow, CSF in light blue, gray matter in gray and white matter is represented by the diffusion tensors of the corrected dMRI data (colors denote direction: green for anterior (A) – posterior (P), blue for superior – inferior and red for left (L) – right (R)). A midsagittal view of the 6C head model is presented in the lower right column where scalp is in leather color, skull compacta in dark gray, skull spongiosa in yellow, CSF in light red, gray matter in orange and white matter in white.

B. Functional Source Separation and Source Analysis

The short temporal components P14, P20/N20 and P25/N25 (15 ms range) are separated individually into functional source (*FS*) using a handmade-developed implementation of the FSS algorithm [15, 16]. Each FS includes enhanced information of a component's functional property. The operation and the parameters for the tuned of FSS are explicitly referred in [17].

Source localization is performed on the back-projected FSs of EMEG modality for every time instant, using the sLORETA algorithm on a skull-conductivity calibrated and white-matter anisotropic realistic head model including six-compartments (scalp, skull compacta and spongiosa, cerebrospinal fluid (CSF), gray and white matter) [6]. The sLORETA estimates the standardized current density for one source point k as [20]:

$$\hat{S}_{MNE_k}^T\{[R]_{kk}\}^{-1}\hat{S}_{MNE_k} \quad (1)$$

with the $\hat{S}_{\mathrm{MNE}}$ is the current density estimate of the minimum norm estimates (MNE) and the R is the covariance of the estimated current density. In order to illustrate the dipole from sLORETA, the Cholesky decomposition is applied on the symmetric inverse R. The covariance matrix R becomes from semi-positive to positive matrix due to the positive regularization parameter of sLORETA. Therefore, by utilizing the Cholesky decomposition, $R^{-1} = A_R A_R^T$, where A_R denotes the Cholesky decomposition matrix. By replacing the new form of R^{-1} to eq. 1, the source $\hat{S}_{sLOR}$ changes to:

$$\hat{S}_{MNE}{}^T A_R A_R^T \hat{S}_{MNE} = \left(A_R^T \hat{S}_{MNE}\right)^T \left(A_R^T \hat{S}_{MNE}\right) = \hat{S}_{sLOR}^T \hat{S}_{sLOR} \quad (2)$$

so as to

$$\hat{S}_{sLOR} = A_R^T \hat{S}_{MNE}$$

The source waveforms and the dipoles were produced by taking the average current density of the 10% of the maximum power. FEM forward simulations were applied through the SimBio toolbox[1]. The conductivities were 0.43 S/m for the scalp, 0.0083 S/m for skull compacta, 0.031 S/m for skull spongiosa, 1.79 S/m for CSF and 0.33 for gray matter and anisotropic white matter conductivity was modeled based on the the dMRI data [21]. The segmented six-compartment head model is presented in Fig. 1. The source space followed the gray matter folding and the sources fulfilled the St. Venant condition [5].

C. Source Connectivity Analysis

We modeled the effective source connectivity between the components of the somatosensory network by using the time-varying GOPDC (tv-GOPDC) [18]. Moreover, the integrated GOPDC (tv-iGOPDC) is calculated across the frequency range of interest (here the entire spectrum) for every time point. The connectivity analysis is applied for the source waveforms of each modality. A slide-window of 10 ms is selected with an overlap of one ms. Each window is fitted to a multivariable model in order to bring out the causalities between the signals in the coefficients matrix $\boldsymbol{A}$, which was calculated using the ARfit toolbox [22]. The tv-GOPDC flows (tv-iGOPDC value) are then calculated. Finally, we statistically filter the resulting flows through an iterative procedure. The procedure produces an empirical distribution of 300 surrogate data from which, we use a CI of 95 % as standard [23] , and test a CI of 90 % of the distribution to assess possible influences on the reconstructed network. A

[1] www.mrt.uni-jena.de/simbio/index.php?title=Main_Page

flow was determined as significant if it was higher than the aforementioned statistical threshold.

III. Results

The averaged SEP/SEF across all trials are presented in Fig. 2 along with the scalp topographies at the latencies of interest. Clear dipolar patterns occurred for the components P20/N20 for both EEG and MEG and for P25/N25 for MEG, while the P14 had a dipolar pattern with large distance between poles, pointing to the higher depth of the underlying source. When comparing the scalp topographies between EEG and MEG, we observe that the EEG topography is less focal and always perpendicular to the MEG one. In addition, the MEG detects only a very weak tangential part of the P14 component, while it strongly (compared to the P14) detects the tangential part of the P25/N25. Due to space-limitation, we do not present the EEG P25/N25.

Fig. 3 illustrates the EMEG source waveforms of the components. Here, it is important to mention that we present sLORETA-based dipoles on the T1 MRI as estimated by eq. (2) and not their distribution. In this manner, we are able to show the orientation of the reconstructed activity for the Thalamic component and for the SI components, which were distributed in the areas 3b and 1 of the primary somatosensory cortex.

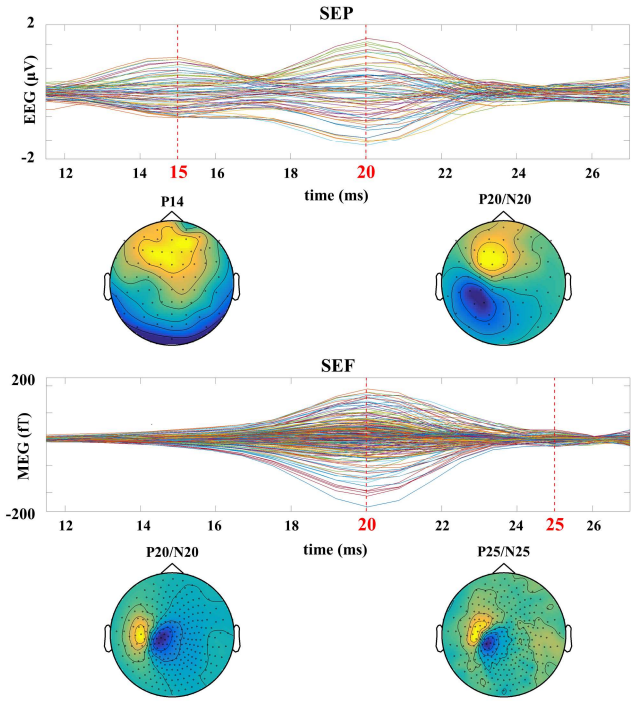

Fig. 2. The averaged SEP (upper row) and SEF (lower row) responses, along with the scalp topographies at the time-points of interest (15, 20 and 25 ms) are presented.

The time-varying connectivity analysis was performed on the source waveforms. Three-time windows were selected to point out the effective connectivity of: $P14 \rightarrow P20/N20$, $P20/N20 \rightarrow P25/N25$ and $P25/N25 \rightarrow P20/N20$.

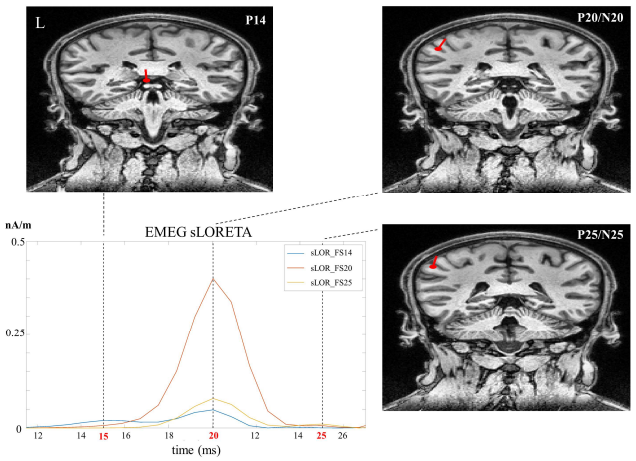

Fig. 3. The EMEG source waveforms (left lower column) with the sLORETA-dipoles (P14: left upper column, P20/N20: right upper column, P25/N25: right lower column) that are visualized on the coronal view of the T1 MRI for each component (P14 at 15 ms, P20/N20 at 20 ms and P25/N25 at 25 ms). The abbreviation L (left) denotes MRI direction.

In Fig. 4, we illustrate the early primary somatosensory network (P14 – P20/N20 – P25/N25) as we dynamically estimated it with the tv-GOPDC metric. In the upper row of the Fig. 4, we present the time-evolution of the flows between the investigated components, while we show the time-stamp interactions on the lower column. We clearly observe (Fig. 4, left lower column) that the P14 contributes to the P20/N20 responses. In the middle lower part of Fig. 4, we also observe that P14 and P20/N20 contribute to the P25/N25. In the right lower column, we detect the opposite (P25/N25→ P20/N20) association, while P14 has no contribution.

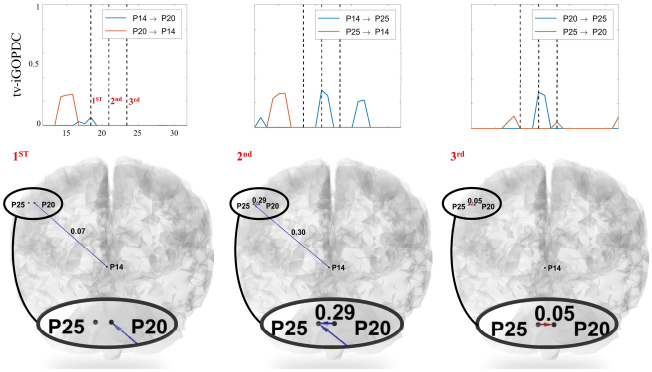

Fig. 4. The tv-iGOPDC forward and backward flows (blue and orange) of each pair of components are shown for 95 % CI. The dash lines illustrate the 1st, 2nd and 3rd time instances in which the causality graphs are illustrated (lower row). These time instances represent the maximum influence of the P14 to P20 (1st), P20 to P25 (2nd) and P25 to P20 (3rd). Only the statistically filtered flows are presented.

In the last figure (Fig. 5), we investigate the influence of the statistical filtering when using a larger CI (i.e., 90 %). In this case, we observe that the network changes compared to the previously presented (Fig. 4), including flows between the investigated components that do not fit to the flow of the neurological activity from the wrist to the somatosensory network.

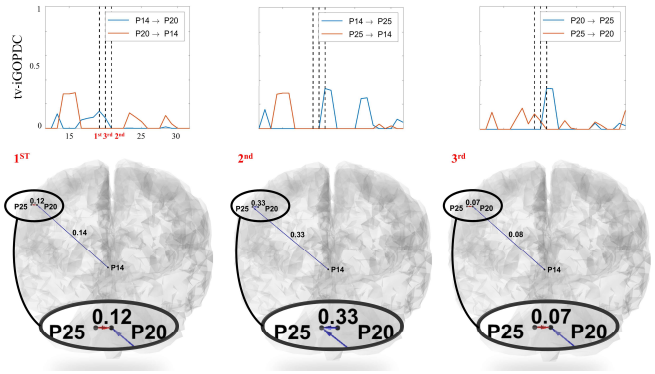

Fig. 5. The tv-iGOPDC forward and backward flows (blue and orange) of each pair of components are shown for 90 % CI. The dash lines illustrate the 1st, 3rd and 2nd time instances in which the causality graphs are illustrated (lower row). These time instances represent the maximum influence of the P14 to P20 (1st), P20 to P25 (2nd) and P25 to P20 (3rd). Only the statistically filtered flows are presented.

IV. Discussion and Conclusion

In the present subject-specific study, we investigated the early primary somatosensory network including the subcortical component P14 and the two transient components P20/N20 and P25/N25. This study was based on our proposed pipeline for connectivity analysis [6, 17]. We used the FSS decomposition algorithm to disentangle the early somatosensory evoked responses into functionally independent components. The realistic and calibrated head model used for source analysis comprised six compartments, brain anisotropy and calibrated skull conductivity. We also exploit the complementarity of EEG and MEG, performing source analysis using their combination (EMEG). In this study, we further investigated the influence of the statistical filtering on the estimation of the causality network.

The estimated locations presented in Fig. 3 are in line with previous well accepted studies [1, 2] in which the authors had estimated the location of all three components using a considerably high number of trials (6000) but simplified head modeling. In this study, the number of trials was significantly smaller (1000), but used high-resolution head modeling with individual and calibrated white matter and skull conductivities.

Our EMEG source network brought together the complementarity of EEG and MEG [12] for modeling the very fast communication within the cortical and subcortical regions involved in the early activated somatosensory. Previous studies, [3, 4] had shown similar interactions, however, in those studies the benefit of EMEG was not utilized. Comparing with other recent studies, the authors in [16] achieved to estimate the somatosensory functional source responses by using FSS on SEF responses. Much later, the study in [15] used the FSS to decompose the early SEP components on the basis of simplified head models with which, the proposed results might be suboptimal due to the vulnerability of the electric potentials to tissue conductivity change [6, 24]. In this study, we showed that FSS was able to derive the investigated components. Furthermore, for first time we also introduce a mathematical representation of modeling the sLORETA current density as a dipole in order to better quantify the orientation component of the estimated activity. We also observed that the use of larger CI in the statistical filtering influences the estimated brain network, leading to possibly noise and unrealistic results (Fig. 5) that do not also fit to the literature [3, 4]. In summary, our study proposes a pipeline to model accurately the very early somatosensory network based on well-parametrized procedures. We also propose an alternative way to present the sLORETA current density as a dipole. For the statistical filtering of the estimated network, as shown (Figs. 4 and 5), we suggest the use of 95 % CI. With this study, we reveal the ability of using EMEG with realistic head modeling and time-varying effective connectivity in order to investigate a very rapid brain network. Even though, further experiments are required, our study supports the notion that network connectivity investigations can profit from EMEG and source analysis with individually skull-conductivity calibrated realistic FEM head models.

Acknowledgments

This research has been co-financed by the European Regional Development Fund of the European Union and Greek national funds through the Operational Program Competitiveness, entrepreneurship and Innovation, under the call RESEARCH CREATE INNOVATE (project code: T1EDK-04440, x-ΒΛΕΨΙΣ). This work was by the "Alexander S. Onassis" Public Benefit Foundation and the German Research Foundation (DFG) in the scope of the priority program SPP1665, project WO1425/5-1.

Reference

[1] H. Buchner, M. Fuchs, H.-A. Wischmann, O. Dössel, I. Ludwig, A. Knepper and P. Berg, "Source analysis of median nerve and finger stimulated somatosensory evoked potentials: multichannel simultaneous recording of electric and magnetic fields combined with 3D-MR," *Brain Tomography,* vol. 6, p. 299–310, 1994.

[2] H. Buchner, T. D. Waberski, M. Fuchs, R. Drenckhahn, M. Wagner and H. A. & Wichmann, "Postcentral origin of P22: evidence from source reconstruction in a realistically shaped head model and from a patient with a postcentral lesion," *Electroencephalography and Clinical Neurophysiology/Evoked Potentials Section,* Vols. 100(4), 332-342, 1996.

[3] J. Haueisen, L. Leistritz, T. Süsse, G. Curio and H. Witte, "Identifying mutual information transfer in the brain with differential-algebraic modeling: Evidence for fast oscillatory coupling between cortical somatosensory areas 3b and 1," *Neuroimage,* Vols. 37(1), 130-136, 2007.

[4] T. Götz, R. Huonker, O. W. Witte and J. Haueisen, "Thalamocortical Impulse Propagation and Information Transfer in EEG and MEG," *Journal of clinical neurophysiology : official publication of the American Electroencephalographic Society,* vol. 31, pp. 253-260 , 2014.

[5] Ü. Aydin, J. Vorwerk, P. Küpper, M. Heers, H. Kugel, A. Galka, L. Hamid, J. Wellmer, C. Kellinghaus, S. Rampp and C. H. Wolters, "Combining EEG and MEG for the reconstruction of epileptic activity using a calibrated realistic volume conductor model," *PLoS One,* vol. 9, no. 3, p. e93154, 2014.

[6] M. Antonakakis, S. Schrader, Ü. Aydin, A. Khan, J. Gross, M. Zervakis, ... and C. H. Wolters, "Inter-subject variability of skull conductivity and thickness in calibrated realistic head models," *NeuroImage,* Vols. 223, 117353, 2020.

[7] M. Antonakakis, S. Schrader, A. Wollbrink, R. Oostenveld, S. Rampp, J. Haueissen and C. H. Wolters, "The effect of stimulation type, head modeling and combined EEG and MEG on the source reconstruction of the somatosensory P20/N20 component," in *Human Brain Mapping accepted for publication, First published: August 2019 https://doi.org/10.1002/hbm.24754.* , 2019.

[8] M. C. Piastra, A. Nüßing, J. Vorwerk, M. Clerc, C. Engwer and C. H. Wolters, "A comprehensive study on electroencephalography and magnetoencephalography sensitivity to cortical and subcortical sources," *Human Brain Mapping,* 2020.

[9] Ü. Aydin, S. Rampp, A. Wollbrink, H. Kugel, J. H. Cho, T. R. Knösche, ... and C. H. Wolters, "Zoomed MRI guided by combined EEG/MEG source analysis: a multimodal approach for optimizing presurgical epilepsy work-up and its application in a multi-focal epilepsy patient case study," *Brain topography,* pp. 30(4), 417-433, 2017.

[10] M. Antonakakis, S. Rampp, C. Kellinghaus, C. H. Wolters and G. Moeddel, "Individualized Targeting and Optimization of Multi-channel Transcranial Direct Current Stimulation in Drug-Resistant Epilepsy," *In BIBE,* pp. 871-876, 2019.

[11] A. Khan, M. Antonakakis, N. Vogenauer, A. Wollbrink, S. Suntrup-Krueger, R. Schneider, S. Herrmann, M. Nitsche, W. Paulus, J. Haueisen and et al., "Constrained maximum intensity optimized multi-electrode tDCS targeting of human somatosensory network," *Conf. Proc. IEEE Eng. Med. Biol. Soc. 2019, 5894-5897. Doi: 10.1109/EMBC.2019.8857253.*

[12] G. Dassios, A. S. Fokas and D. Hadjiloizi, "On the complementarity of electroencephalography and magnetoencephalography," *Inverse Problems,* vol. 23, no. 6, p. 2541–2549, 2007.

[13] M.-X. Huang, T. Song, D. Hagler, I. Podgorny, V. Jousmaki, L. Cui, K. Gaa, D. Harrington, A. Dale, R. Lee and et al., "A novel integrated MEG and EEG analysis method for dipolar sources," *NeuroImage 2007, 37, 731–748, doi:10.1016/j.neuroimage.2007.06.002.*

[14] H. McCann, G. Pisano and L. Beltrachini, "Variation in Reported Human Head Tissue Electrical Conductivity Values," *Brain topography 2019, 32, 825–858, doi:10.1007/s10548-019-00710-2.*

[15] C. Porcaro, G. Coppola, F. Pierelli, S. Seri, G. D. Lorenzo, L. Tomasevic, C. Salustri and F. Tecchio, "Multiple frequency functional connectivity in the hand somatosensory network: An EEG study," *Clinical Neurophysiology,* vol. 124, p. 1216–1224, 2013.

[16] G. Barbati, R. Sigismondi, F. Zappasodi, C. Porcaro, S. Graziadio, G. Valente, M. Balsi, P. M. Rossini and F. Tecchio, "Functional source separation from magnetoencephalographic signals," *Human Brain Mapping,* vol. 27, pp. 925-934, 2006.

[17] K. Politof, M. Antonakakis, A. Wollbrink, M. E. Zervakis and C. H. Wolters, "Effective Connectivity in the Primary Somatosensory Network using Combined EEG and MEG," in *IEEE 19th International Conference on BIBE, Athens, Greece, 2019, pp. 593-597, doi: 10.1109/BIBE.2019.00113.*

[18] A. Omidvarnia, G. Azemi, B. Boashash, J. M. O. Toole, P. Colditz and S. Vanhatalo, "Measuring Time-Varying Information Flow in Scalp EEG Signals: Orthogonalized Partial Directed Coherence," *IEEE Transactions on Biomedical Engineering,* vol. 61, no. 3, pp. 680-693, 2013.

[19] R. Oostenveld, P. Fries, E. Maris and J. M. Schoffelen, "FieldTrip: Open source software for advanced analysis of MEG, EEG, and invasive electrophysiological data," *Computational Intelligence and Neuroscience,* Vols. vol. 2011, Article ID 156869, 2011.

[20] R. Grech, T. Cassar, J. Muscat, K. P. Camilleri, S. G. Fabri, M. Zervakis, ... and B. Vanrumste, "Review on solving the inverse problem in EEG source analysis," *Journal of neuroengineering and rehabilitation,* Vols. 5(1), 25, 2008.

[21] D. Tuch, V. J. Wedeen, A. M. Dale, J. S. George and J. W. Belliveau, "Conductivity tensor mapping of the human brain using diffusion tensor MRI," *Proceedings of the National Academy of Sciences,* vol. 98, no. 20, pp. 11697-701, 2001.

[22] T. Schneider and A. Neumaier, "Algorithm 808: ARfit - a MATLAB package for the estimation of parameters and eigenmodes of multivariate autoregressive models," *ACM Transactions on Mathematical Software,* 2000.

[23] M. Antonakakis, G. Giannakakis, M. Tsiknakis, S. Micheloyannis and M. Zervakis, "Synchronization coupling investigation using ICA cluster analysis in resting MEG signals in reading difficulties," *In 13th IEEE International Conference on BioInformatics and BioEngineering,* pp. 1-5, 2013.

[24] J. Vorwerk, Ü. Aydin, C. Wolters and C. Butson, "Influence of Head Tissue Conductivity Uncertainties on EEG Dipole Reconstruction," *Frontiers in Neuroscience,* 2019.